Hydrology and Earth System Sciences Discussions

Geomorphometry of drainage basins: a global view from the Shuttle Radar Topography Mission

P. L. Guth

Department of Oceanography, US Naval Academy, Annapolis, MD, USA

Correspondence to: P. L. Guth (pguth@usna.edu)

HESSD

8, 1929–1949, 2011

Geomorphometry of drainage basins

P. L. Guth

Full Screen / Esc

Printer-friendly Version

Interactive Discussion

Abstract

A suite of 42 geomorphometric parameters for each of 26 272 drainage basins larger than 100 km^2 from the Hydrosheds Shuttle Radar Topography digital elevation model shows the global distribution of Strahler order for streams and drainage basins; the largest basins are order 9. Many common parameters depend both on the size of the basin, and the scale of the digital elevation model used for the computations. These drainage basins display the typical longitudinal stream profiles, but the major basins tend to be more convex than the smaller basins.

1 Introduction

The Shuttle Radar Topography Mission (SRTM) created a near global digital elevation model (DEM) with 3 arc second spacing, about 90 m (Farr et al., 2007). Despite some voids in mountainous terrain and sandy desert regions, the SRTM DEM remains the best freely available dataset and several projects have worked to fill the voids (Jarvis et al., 2008; Lehner et al., 2008a, b). The SRTM's greatest weakness is the lack of coverage for Antarctica and latitudes north of 60°.

The Hydrosheds project (Lehner et al., 2008a, b) created a hole-filled version of the SRTM DEM, conditioned the dataset for hydrologic applications, and released a drainage network and basins outlines from a 15 arc second version of SRTM. This data set includes 3.46 million stream segments in 2.48 million basins; most of the basins are small and contain at most one stream segment. A segment connects two nodes, with a node being either the terminus of a segment or the junction of two segments. The largest 1.06% of the basins, those over 100 km^2 in area, contain 98.64% of the stream segments.

Geomorphometry performs quantitative land-surface analysis (Pike et al., 2009), and the SRTM data provides a data set at an appropriate scale for global analyses. Guth (2006) looked at 12 key geomorphometric parameters from SRTM to compare

results with the US National Elevation Dataset, and further described 30 parameters computed worldwide from SRTM (Guth, 2009). Those analyses used small rectangular areas (0.5 million in the United States, 7.4 million in the entire world) which can be considered random sampling areas.

⁵ This study seeks to use the Hydrosheds drainage basins, natural sampling areas of varying size, and computes both geomorphometric parameters from the DEM, metrics of the drainage basin and channel networks, and characteristics of the channel thalwegs.

2 Methods and limitations

¹⁰ Appendix A lists the processing steps used with the Hydrosheds data. I excluded basins with an area less than $100 \, \text{km}^2$. With the $15''$ DEM used to compute the drainage network, each pixel is about $464 \times 461 \, \text{m}$ at the equator and $232 \times 464 \, \text{m}$ at $60°$, the limit of the SRTM data. These represent about $0.2 \, \text{km}^2$ and $0.1 \, \text{km}^2$ respectively, so a $100 \, \text{km}^2$ drainage basin contains 500–1000 elevation points. These basins ¹⁵ are likely to have only a single channel, and produce statistics of limited validity. While this size limit is somewhat arbitrary, over 85% of the drainage basins identified by Hydrosheds have areas less than $1 \, \text{km}^2$ and most of these have no channel segments. Most of these small basins occur on the coastline, or large areas of interior drainage (Fig. 1).

²⁰ The scale of the DEM used to create the drainage network limits the scale of features visible in the drainage networks. The smallest segments will be a single pixel, about a half kilometer, and will influence parameters like sinuosity, so care must be taken in comparing these results with those from different scales.

Computed thalwegs (the major channel in the basin) are based solely on landforms ²⁵ in the SRTM data, and not on hydrology; some channels might be intermittent or almost always dry. The thalwegs start from the last river segment in the basin, which has the largest contributing area and no downstream connections. I trace the thalweg

upstream, at each junction taking the tributary with the larger contributing area. This algorithm can be fooled in cases where climate does not produce rainfall and runoff proportional to area; the Nile, highlighted in Fig. 1, shows the computed thalweg following the Bahr el Ghazal and Bahr al-Arab west into Darfur, tributaries of the White
5 Nile, instead of following the water up the Blue Nile. The number of basins in the data set precludes a manual search to correct this limitation.

Figure 2 compares the Hydrosheds drainage network with the medium resolution network from the US National Hydrography Dataset (NHD; Simley and Carswell, 2009). At regional scales they line up very well, and because the NHD reflects a larger scale, it
10 generally shows additional tributaries. The number of additional tributaries varies with landforms and the resulting channel patterns. Brief qualitative assessment suggests that the Strahler order 1 streams in this region range from order 1 to 4 in the NHD data, and most commonly are order 2 or 3. Figure 2 also shows the bimodal distribution of small basins ($<100\,\mathrm{km}^2$): a great many tiny basins along the coast with no stream seg-
15 ments, and a much smaller number of first and some second order drainage networks between the outlets of the larger basins.

3 Results

Figure 3 shows the drainage basins coded by Strahler order. The three largest streams on earth (Amazon, Congo, and Volga) have a Strahler order of 9, and very different
20 geomorphic regimes due to significant differences in total basin relief (6211, 3955, and 1624 m respectively). Figure 4 shows a histogram of Strahler order for the 26 272 basins with an area greater than $100\,\mathrm{km}^2$, clearly demonstrating a logarithmic decline in the number of basins with increasing order. Limiting basin size to $100\,\mathrm{km}^2$ removes many small order 1 streams; an alternative might be to restrict analysis to order 2 and
25 larger streams.

Figure 5 shows maps color-coded by 4 of the basin geomorphometric parameters listed in Appendix B. Like Fig. 3, the map visually emphasizes the large basins. On

all of these maps, several characteristics stand out. The desert belts (North American Great Basin, Sahara, Arabian peninsula, central Asia, and western Australia) tend to lack large drainage basins, in both area and Strahler order. ELEV_RELF (Fig. 5a) is the elevation-relief ratio computed from the DEM. The Dnieper River basin has the largest value of this parameter, due to an elevation distribution with almost all the points in the middle of the elevation distribution and very little area near the elevation of the Black Sea, and a thalweg which descends comparatively rapidly near its mouth at the Black Sea. Figure 5b shows the RATIO_RELF parameter, which considers only the geometry of the thalweg and in essence computes its average slope. The largest values occur in small steep basins which do not show up well at this scale; of major rivers, the largest values are from the Mekong and Yangtze, which have thalwegs that ascend high into the central Asian mountains. Figure 5c shows BASIN_RUGD, which is the ratio of basin's elevation range to its area, and this metric rewards small, steep basins along coasts and interior basins in central Asia; coloring by the logarithm emphasizes the huge range in values for this parameter, from nearly 0 for very large, flat basins to 36 for small steep basins. Figure 5d shows basin SINUOSITY, with low values for a straight thalweg and higher values for curved channels. The most sinuous major river that appears at this scale is the Don, which curves 1896 km to travel a straight line distance of 521 km.

Figures 6 and 7 look at basin thalwegs, on a normalized plot of elevation and distance so that profile shapes can be compared. Figure 6 contours the density of thalweg shapes, in terms of the percentage of basin in each percent on the graph. Densities less than 1 are not shown, and the magenta includes values significantly larger than 5. Profiles tend to be very gentle near the mouth of the river, and steep near the headwaters, reflecting the traditional graded profile. The small basins, which dominate Fig. 6a, tend to have a much more linear profile; the larger streams tend to have a flatter downstream segment, steeper headwaters, and an overall more concave profile as seen in Fig. 6b. Figure 7 shows the thalwegs of the 25 largest basins (defined as having over 500 m relief along the thalweg, and Strahler order 8 or 9). The graphs exhibit

Title Page

Abstract | Introduction

Conclusions | References

Tables | Figures

Back | Close

Full Screen / Esc

Printer-friendly Version

Interactive Discussion

noise in the measured elevations where the channel goes through deep canyons; we are working on a satisfactory automatic filtering algorithm that will work with all 26 272 thalwegs. A number of the thalwegs in Fig. 7 lie outside the common zones seen in Fig. 6; for example, both the Amazon and Niger (Fig. 7b) have extremely steep
5 headwaters, while the Nelson has an extremely abrupt descent into Hudson's Bay, as well as much lower overall relief compared to the others in this group. Several of these thalwegs, such as the Indus, show several distinct convex segments.

Figure 8 shows a correlation matrix for the 42 parameters in Appendix B, for all 26 272 basins. Blue represents the strength of positive correlations, and red negative corre-
10 lations. Positive correlations >0.90 mostly demonstrate that many of the parameters really reflect different ways of expressing slope; the one correlation that is not directly related to slope is a high correlation between the log of the basin area and the Strahler order. The strongest negative correlations are for S2S3 and STRENGTH, negatively correlated with the slope measures because they are defined as inverse slope mea-
15 sures.

4 Discussion

Wechsler (2007) looked at uncertainties in DEMs and how they impacted hydrologic applications. He emphasized that the results of using DEMs depended on both the DEM quality, and its scale. The results reported here rely on 15″ data, appropriate for
20 global analysis, but could be extended to 3″ scale by using the full resolution of the SRTM data. The most significant problem will be the holes in the data, and lack of coverage at high northern latitudes, but the SRTM appears to be the best candidate for a global dataset for the immediate future. Initial claims for the superiority of the 1″ ASTER GDEM do not appear to be substantiated (Guth, 2010), and even the 1″
25 SRTM data currently restricted to the United States military and publicly available only for the continental United States does not provide much improvement over the 3″ data for geomorphometry (Guth, 2006).

Despite the limitations of scale and data quality, the SRTM drainage data provides a real bonanza for quantitative geomorphology. The challenge will be to frame the correct comparisons, which will probably involve restricting analysis to basins with similar size or Strahler order, and looking at the subbasins within the global data set. The elevation data from SRTM consists of about 35 GB of data, and cheap processing and storage allows manipulation on common desktop computers.

5 Conclusions

The SRTM-derived Hydrosheds data set contains 26 272 basins with an area greater than 100 km^2, and provides a near-global, internally consistent data set to investigate the gemorphological properties of both the basin and the thalweg profiles. The current resolution of this data is 15$''$ (about 0.5 km), appropriate for global studies. Because most parameters depend on the scale of the data used for computations, these results cannot be readily compared to other studies. Parameters also depend on the size of the drainage basin as well as the resolution of the input data, but the SRTM data provides a fascinating picture of the world's drainage patterns.

Appendix A

Processing steps

1. Create a basin identifier for each basin, which combines the basin number from Hydrosheds with a two digit code for the continent, which allows linking the data sets for each basin and looking at multiple continents simultaneously.

2. Remove basins with areas less than 100 km^2 from the 15$''$ Hydrosheds database. This reduced the 2.48 million basins in the original data set to 26 272.
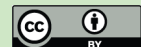
Full Screen / Esc

Printer-friendly Version

Interactive Discussion

3. Create a DEM for each basin, using 6″ SRTM data created by decimating the 3″ Hydrosheds void-filled data. This size allows in memory manipulation of the largest drainage basins for fast processing, and is still higher resolution than the drainage basins.

4. Assign each drainage segment to a basin using a point in area function; segments in the small drainage basins are left unassigned.

5. Extract nodes and create topology for each basin from the nodes at the end of each drainage segment, and compute its Strahler order

6. Create thalweg for each basin as a 3-D shapefile with the elevations from the 15″ Hydrosheds DEM (6″ DEM produces similar results).

7. Compute geomorphometric parameters listed in Appendix B for each drainage basin.

8. Modify Hydrosheds river files to include the basin to which it belongs, its Strahler order, and whether it lies on the thalweg of the drainage system.

9. Modify the Hydrosheds basin files to include Strahler order, the total length of channels in the basin, the length of the thalweg, and the perimeter of the basin.

10. Manually identify significant basins by reference to atlases and other reference material.

Appendix B

Geomorphometric parameters

1. NPTS: number of points in drainage basin (6″ DEM).

2. ELEV_AVG: average elevation (6″ DEM).

3. ELEV_STD: standard deviation of elevation (6″ DEM).

4. ELEV_SKW: skewness of elevation (6″ DEM).

5. ELEV_KRT: kurtosis of elevation (6″ DEM).

6. RELIEF: elevation range [MaxZ – MinZ] (6″ DEM).

7. ELEV_MAX: maximum elevation (6″ DEM).

8. ELEV_RELF: Elevation-relief ratio or coefficient of dissection
   ([ELEV_AVG – Min Elevation]/RELIEF)
   (Pike and Wilson, 1971; Etzelmuller, 2000; Strahler, 1952).

9. SLOPE_MAX: maximum slope in percent (6″ DEM). Slope computed with Evans (1998) method, modified for DEM spacing in arc seconds.

10. SLOPE_AVG: Steepness or Roughness, average slope (6″ DEM).

11. SLOPE_STD: standard deviation of slope (6″ DEM).

12. SLOPE_SKW: skewness of slope (6″ DEM).

13. SLOPE_KRT: kurtosis of slope (6″ DEM).

14. S1S2: flatness, or slope inverse (Guth, 2003).

Geomorphometry of drainage basins

P. L. Guth

15. S2S3: terrain organization (Guth, 2003). High values correlate with strong tendency for ridges and valleys to align.

16. STRENGTH: alternate formulation for flatness (Fisher et al., 1987, p. 48, 159).

17. SHAPE: alternate formulation for terrain organization (Fisher et al., 1987, p. 48, 159).

18. ROUGHNESS: strong correlation with slope (Mark, 1975; Etzelmuller, 2000).

19. PROFC_AVG: average profile curvature ($6''$ DEM). Computed with equations in Wood (1996) based on earlier suggestions from Evans.

20. PROFC_STD: standard deviation of profile curvature ($6''$ DEM).

21. PROFC_SKW: skewness of profile curvature ($6''$ DEM).

22. PROFC_KRT: kurtosis of profile curvature ($6''$ DEM).

23. PLANC_AVG: average plan curvature ($6''$ DEM). Computed with the equations in Wood (1996) based on earlier suggestions from Evans.

24. PLANC_STD: standard deviation of plan curvature ($6''$ DEM).

25. PLANC_SKW: skewness of plan curvature ($6''$ DEM).

26. PLANC_KRT: kurtosis of plan curvature ($6''$ DEM).

27. GAMMA_EW: Nugget variance from the variogram (Curran, 1988), east-west direction. This measures the elevation difference from each point to its nearest neighbor; smaller values reflect smooth terrain, and high values rougher terrain ($6''$ DEM)

28. GAMMA_NS: Nugget variance, north-south direction.

29. GAMMA_NESW: Nugget variance, northeast-southwest direction.

30. GAMMA_NWSE: Nugget variance, northwest-southeast direction.

31. SLP_OV_30: percentage of drainage basin with slope exceeding 30% (6″ DEM).

32. SLP_OV_50: percentage of drainage basin with slope exceeding 50% (6″ DEM).

33. AREA_SQKM: basin area.

34. THALWEG_KM: length of the basin's thalweg.

35. CHANNEL_KM: total length of channels in drainage basin.

36. RELIEF_TH: difference in elevation (m) along the basin thalweg.

37. BASIN_RUGD: RELIEF (m)/AREA_SQKM

38. LOG_RUGD: log base 10 of BASIN_RUGD

39. RATIO_REL: RELIEF_TH (m)/THALWEG_KM

40. STRAHLER_O: Strahler order (Strahler, 1957) computed from the 15″ drainage network. Sometimes called the Strahler-Horten order.

41. PERIMTR_KM: perimeter of 15″ drainage basin.

42. SINUOSITY: ratio of thalweg length to straight line distance connecting thalweg endpoints.

Printer-friendly Version

Interactive Discussion

References

Curran, P. J.: The semivariogram in remote sensing: an introduction, Remote Sens. Environ., 24, 493–507, 1988.

Etzelmuller, B.: On the quantification of surface changes using grid-base digital elevation models (DEMs), Transactions in GIS, 4, 129–143, 2000.

Evans, I. S.: What do terrain statistics really mean?, in: Landform monitoring, modelling and analysis, edited by: in Lane, S. N., Richards, K. S., and Chandler, J. H., J. Wiley, Chichester, 119–138, 1998.

Farr, T. G., Rosen, P. A., Caro, E., Crippen, R., Duren, R., Hensley, S., Kobrick, M., Paller, M., Rodriguez, E., Roth, L., Seal, D., Shaffer, S., Shimada, J., Umland, J., Werner, M., Oskin, M., Burbank, D., and Alsdorf, D.: The shuttle radar topography mission, Rev. Geophys., 45, doi:10.1029/2005RG000183, 2007.

Fisher, N. L, Lewis, T., and Embleton, B. J. J.: Statistical analysis of spherical data, Cambridge University Press, 330 p, 1987.

Guth, P. L.: Terrain organization calculated from digital elevation models, in: Concepts and Modelling in Geomorphology: International Perspectives, edited by: Evans, I. S., Dikau, R., Tokunaga, E., Ohmori, H., and Hirano, M., Terrapub Publishers, Tokyo, 199–220, available at: http://www.terrapub.co.jp/e-library/ohmori/pdf/199.pdf, 2003.

Guth, P. L.: Geomorphometry from SRTM: Comparison to NED, Photogramm. Eng. Rem. S., 72, 269–277, 2006.

Guth, P. L.: Geomorphometry in MICRODEM, in: Geomorphometry: concepts, software, applications, edited by: Hengl, T. and Reuter, H. I., Developments in Soil Science Series, Elsevier, Amsterdam, 351–366, 2009.

Guth, P. L.: Geomorphometric comparison of ASTER GDEM and SRTM, ASPRS/CaGIS, 2010 Fall Specialty Conference, Orlando, FL, November 15–19, Conference CD-ROM, 2010.

Jarvis, A., Reuter, H. I., Nelson, A., and Guevara, E.: Hole-filled SRTM for the globe Version 4, available from the CGIAR-CSI SRTM 90m Database, available at: http://srtm.csi.cgiar.org, 2008.

Lehner, B., Verdin, K., and Jarvis, J.: New global hydrography derived from spaceborne elevation data, EOS, 89, 93–94, 2008a.

Lehner, B., Verdin, K., and Jarvis, J.: HydroSHEDS Technical Documentation Version 1.1, available at: http://gisdata.usgs.gov/webappcontent/HydroSHEDS/downloads/

HydroSHEDS_TechDoc_v11.pdf, 2008b.

Mark, D. M.: Geomorphometric parameters: A review and evaluation, Geografiska Annaler, 57A, 165–177, 1975.

Pike, R. J. and Wilson, S. E.: Elevation-relief ratio, hypsometric integral and geomorphic area-altitude analysis, Geol. Soc. Am. Bull., 82, 1079–1084, 1971.

Pike, R. J., Evans, I. S., and Hengl, T.: Geomorphometry: A brief guide, in: Geomorphometry: concepts, software, applications, edited by: Hengl, T. and Reuter, H. I., Developments in Soil Science Series, Elsevier, 1–30, 2009.

Simley, J. D. and Carswell Jr., W. J.: The National Map – Hydrography, US Geological Survey Fact Sheet 2009–3054, p. 4, available at: http://pubs.usgs.gov/fs/2009/3054/, 2009.

Strahler, A. N.: Hypsometric (area-altitude) analysis of erosional topography, Geol. Soc. Am. Bull., 63, 1117–1142, 1952.

Strahler, A. N.: Quantitative analysis of watershed geomorphology, Transactions of the American Geophysical Union, 8, 913–920, 1957.

Wechsler, S. P.: Uncertainties associated with digital elevation models for hydrologic applications: a review, Hydrol. Earth Syst. Sci., 11, 1481–1500, doi:10.5194/hess-11-1481-2007, 2007.

Wood, J. D.: The geomorphological characterisation of digital elevation models: unpublished PhD Thesis, University of Leicester, UK, available at: http://www.soi.city.ac.uk/~jwo/phd/, 1996.

Geomorphometry of drainage basins

P. L. Guth

Title Page

Abstract	Introduction
Conclusions	References
Tables	Figures

◄ | ►|

◄ | ►

Back | Close

Full Screen / Esc

Printer-friendly Version

Interactive Discussion

Full Screen / Esc

Printer-friendly Version

Interactive Discussion
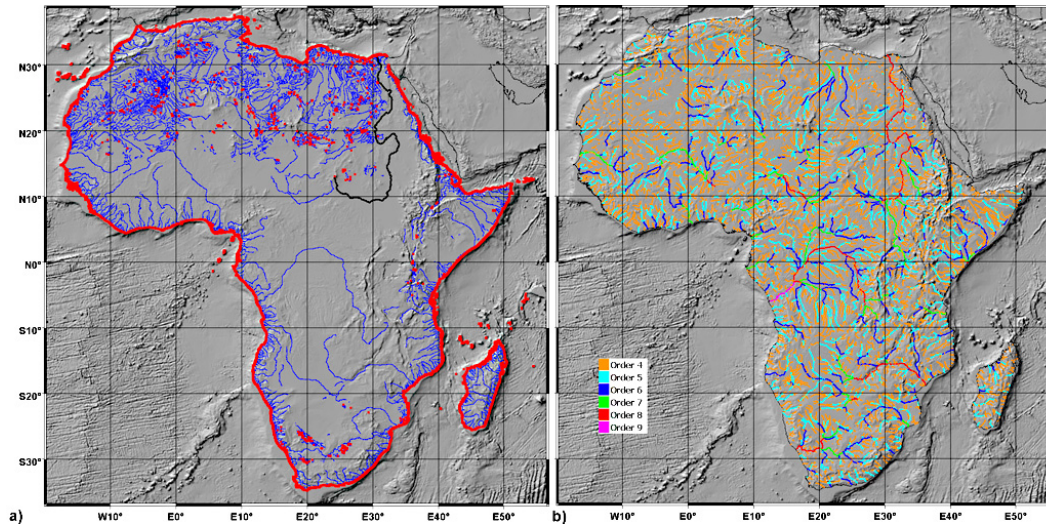
Fig. 1. (a) Red symbols mark drainage basins smaller than 100 km^2 for Africa, with the thalwegs of the larger drainage basins shown in blue. The Nile is highlighted in black. The small basins effectively mark the coastline, with smaller numbers in interior drainage areas such as the Sahara. The size of the symbols greatly exaggerates the importance of the small basins. **(b)** Strahler order for the larger channels in Africa, down to order 4.
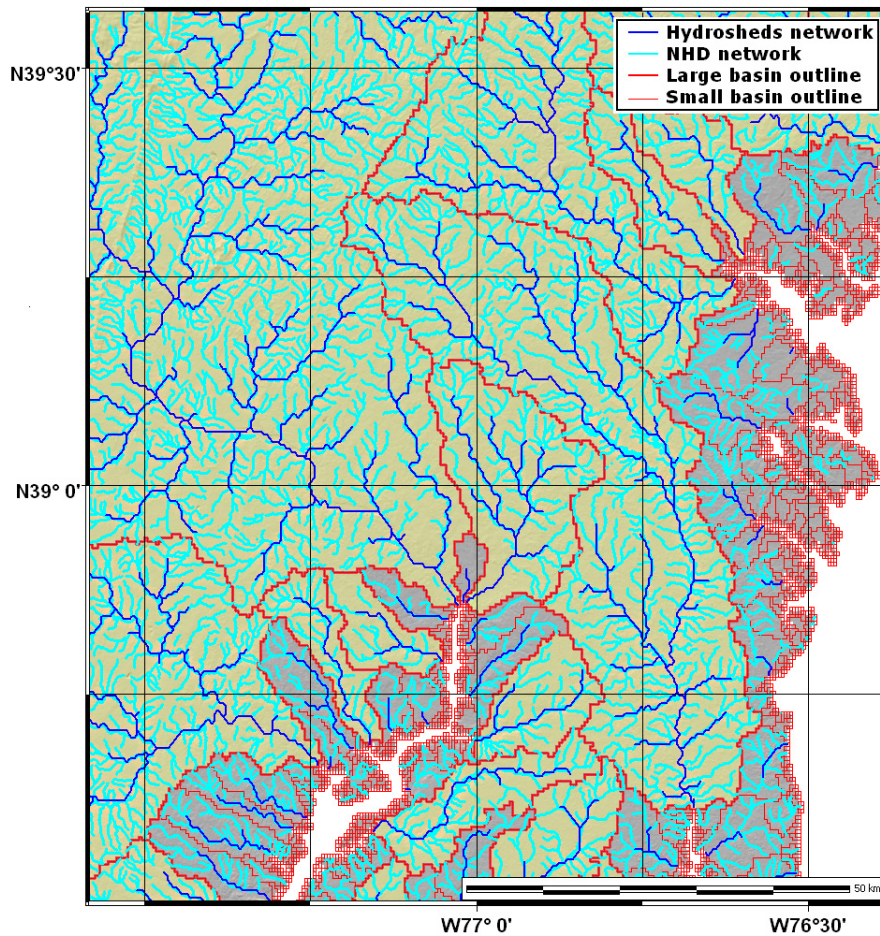
Fig. 2. Comparison of Hydrosheds and NHD drainage networks for part of the Chesapeake Bay watershed.

Fig. 3. Strahler order for the largest segment in global drainage basins.
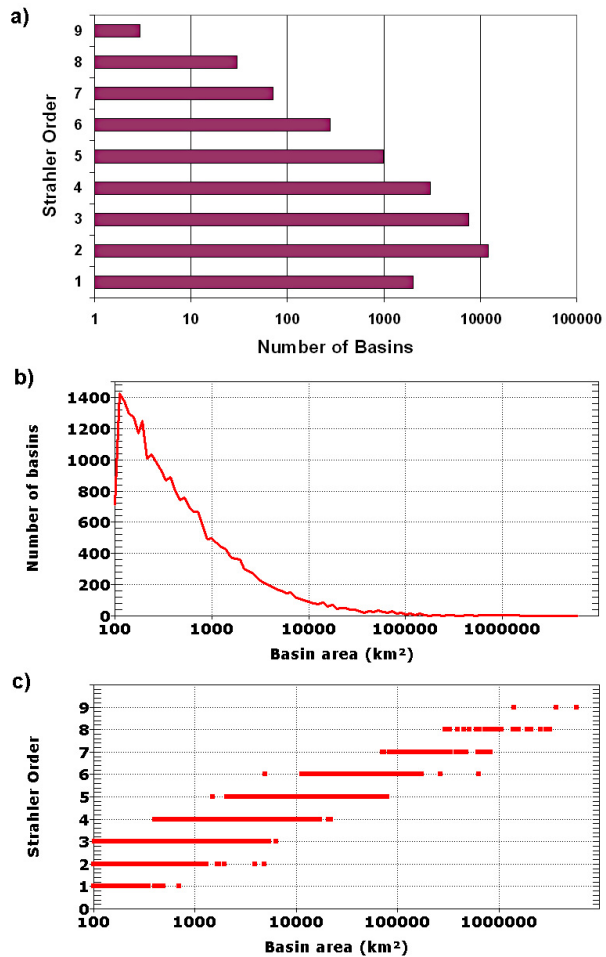
Fig. 4. (a) Histogram of Strahler order. **(b)** Histogram of basin area. **(c)** Basin area (log scale) versus Strahler order.
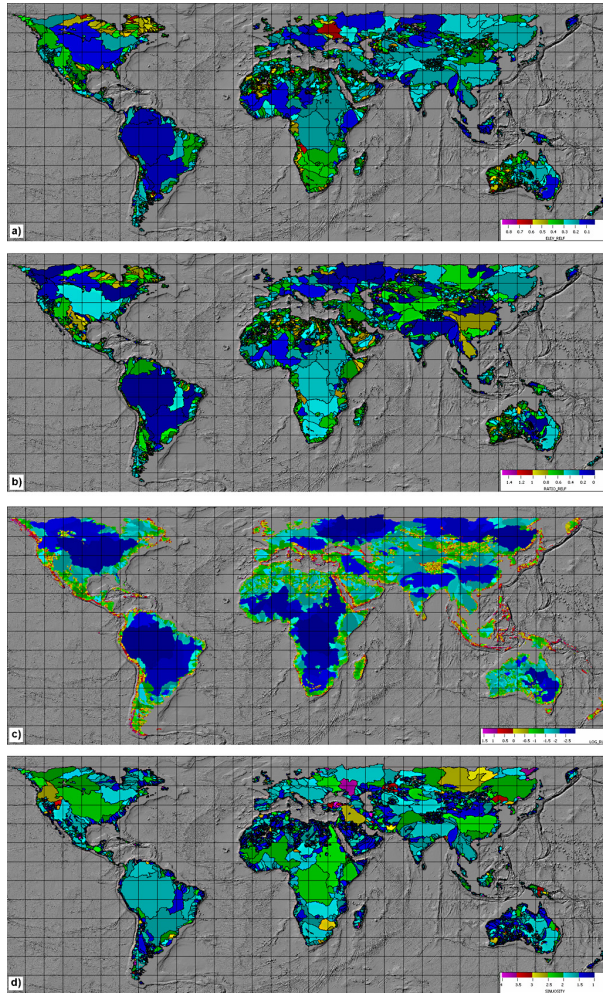
Fig. 5. Maps with drainage basin parameters. **(a)** ELEV_RELF, **(b)** RATIO_RELF, **(c)** LOG_RUGD, and **(d)** SINUOSITY.

Fig. 6. Normalized longitudinal thalweg profiles for all basins **(a)** and those of Strahler order 4 and larger **(b)**. Colors range from 1% (blue) to 5% or greater (violet). Note the displacement downward and to the right for the larger basins.
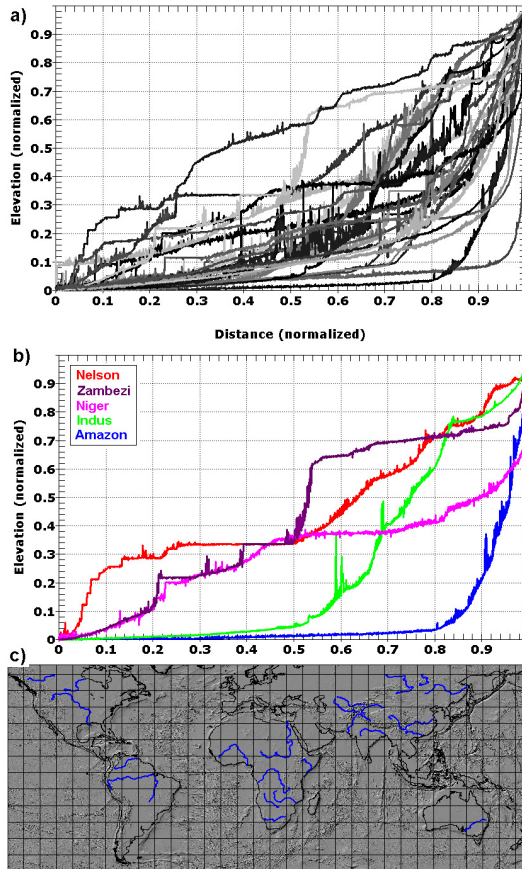
Fig. 7. Thalwegs for the 25 largest global drainage basins (thalweg relief >500 m, Strahler order >= 8): **(a)** normalized basin profiles for all 25 thalwegs; **(b)** labeled thalwegs for 5 channels; **(c)** locations for the thalwegs. Elevation spikes result from using the 6″ DEM instead of the hydrologically conditioned 15″ DEM used to compute the drainage basins.

Fig. 8. Correlation matrix for the parameters in Appendix B for all drainage basins larger than 100 km^2.

Title Page

Abstract | Introduction

Conclusions | References

Tables | Figures

Back | Close

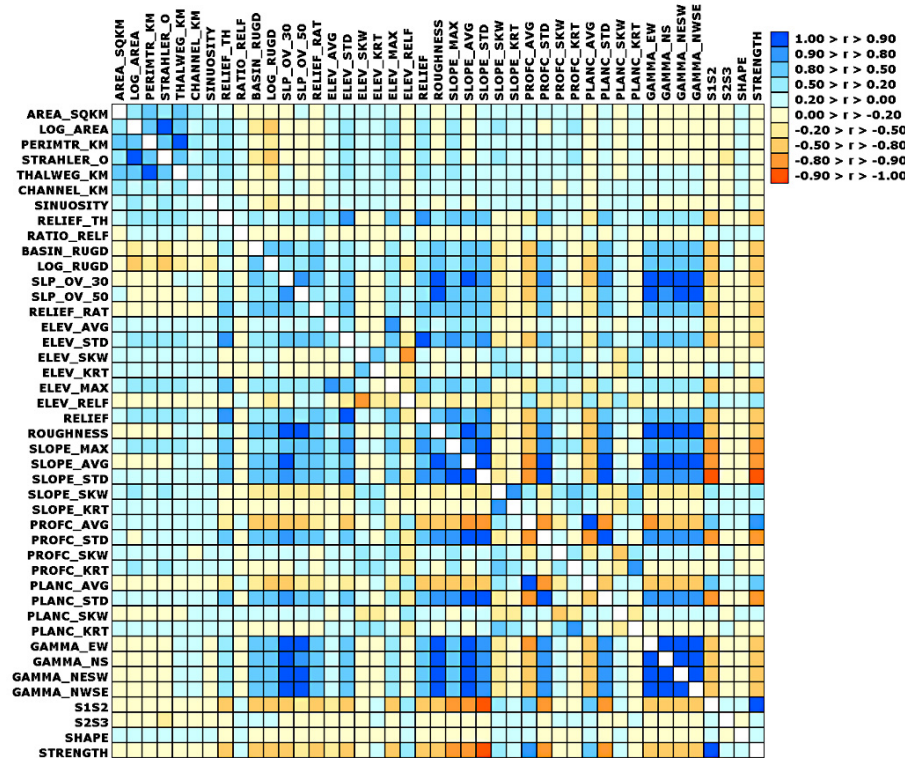Full Screen / Esc

Printer-friendly Version

Interactive Discussion